Climate Defined but Not Soil-restricted: The Distribution of a Neotropical tree through Space and Time

Facundo Alvarez (facualva87@gmail.com)
UNEMAT https://orcid.org/0000-0002-7095-9570
Paulo S Morandi
UNEMAT: Universidade do Estado de Mato Grosso
Ben Hur Marimon-Junior
UNEMAT: Universidade do Estado de Mato Grosso
Reginal Exavier
Universidade Federal de São Paulo: Universidade Federal de Sao Paulo
Igor Araújo
UNEMAT: Universidade do Estado de Mato Grosso
Lucas H Mariano
UNEMAT: Universidade do Estado de Mato Grosso
Angelica Oliveira Muller
UNEMAT: Universidade do Estado de Mato Grosso
Ted R Feldpausch
University of Exeter College of Life and Environmental Sciences
Beatriz Schwantes Marimon
UNEMAT: Universidade do Estado de Mato Grosso

Research Article

Keywords: species distribution models, Amazonia-Cerrado transition, spatial hierarchy

Posted Date: April 19th, 2021

DOI: https://doi.org/10.21203/rs.3.rs-333060/v1

Version of Record: A version of this preprint was published at Plant and Soil on November 10th, 2021. See the published version at https://doi.org/10.1007/s11104-021-05202-6.

Abstract

Aims

Brosimum rubescens, a tree species with a Neotropical distribution, can achieve local monodominance in Southern Amazonia forests. Understanding how and why this species varies across space and time is important because the monodominance of some species alters ecosystems complexity. Here we evaluate the fundamental ecological niche of *B. rubescens* by species distribution models (SDM), combining predictive environmental variables with occurrence points. We specifically aim to 1) determine how the spatial distribution patterns of *B. rubescens* vary with different environmental predictive variables, and 2) evaluate the temporal and spatial persistence of *B. rubescens* in the Neotropics.

Methods

To generate the SDMs, the predictive environmental variables were incorporated as main components of climatic, hydric and soil variables.

Results

All algorithms show higher performance in spatial predictions for hydric variables and for the combination of climatic, hydric and edaphic variables. We identified that the potential niches of *B. rubescens* seem to be defined by climatic fluctuations, with the edaphic conditions being predictive variables that are not restrictive of their presence on the evaluated spatial scale. From the LMG (Last Glacial Maximum) to the present, the species seems to have increased its spatial amplitude; however, from the present to the future, predictions suggest that *B. rubescens* will experience a considerable loss of its range.

Conclusions

Our findings show the independent and combined effects of different environmental variables, allowing us to identify which limit or facilitate the spatial distribution of *B. rubescens*. We corroborate the spatial persistence and geographical fidelity of the species' spatial patterns over time.

Introduction

The global distribution of biodiversity follows a general pattern of spatial radiation from tropics to polar latitudes, and tropical forests are no exception to this spatial pattern (Wiens and Donoghue 2004; Murphy and Bowman 2012). Within this spatial radiation, some tropical tree species dominate 50 to 100% of the total biomass forming what are called monodominant forests (Hart et al. 1989). The monodominance of some species creates complex ecosystems, with no single or independent physical, chemical, or biological mechanism to explain the dominance over space and time (Torti et al. 2001; Peh et al. 2011; ter Steege et al. 2019). The mechanisms that promote and maintain monodominant forests remain poorly understood. One study suggested that those unique communities are associated with hydric, edaphic, and ecological traits occurring together (i.e. shade tolerance, slow decomposition rate, mast seeding, large seeds and poor dispersal, herbivore avoidance, ectomycorrhizal associations) under low exogenous disturbance over long periods (Peh et al. 2011).

Restrictive climatic conditions don't condition the occurrence and monodominance of Neotropical forests, but differences in the distribution of light and the species-specific use capacities of this resource are one major factor for the structuring of such forests (Marimon et al. 2008; Peh et al. 2011). Regarding edaphic factors, neo- and paleo-tropical monodominant forests share some common characteristics, such as poor nutrient availability or excess of certain elements (Marimon et al. 2001; Marimon-Junior 2007; Peh et al. 2011; Elias et al. 2018; Marimon-Junior et al. 2019). Notwithstanding, no evidence exists that soil properties are determinants to create or maintain monodominance (Brito-Rocha et al. 2016; Elias et al. 2018; Marimon-Junior et al. 2019). Modeling the spatial distribution of monodominant species, using different environmental variables and different temporal projections, allows a better understanding of their combined and independent space-temporal effects and a better approximation to their Grinnellian niche.

Brosimum rubescens Taub. (Moraceae), the focal species of the present study has a Neotropical distribution and is associated with non-seasonally flooded tropical forests, with the dispersion center in the Amazon Basin and Guyana, with some records in Central America and Caribe (Berg 1972; Palacios 2005). Moreover, in the Amazonia-Cerrado transition, *B. rubescens* can form monodominant forests of up to 5,000 ha (Marimon et al. 2001), and some studies have shown that this species dominance can reach up to 85% of all trees >10 cm diameter, hence one of the highest values recorded for a Neotropical monodominant species (Marimon et al. 2001). In addition, the high density of *B. rubescens* affects species diversity, unbalancing the uniformity of their abundance by acting as a biological barrier (Marimon-Júnior, 2007; Marimon *et al*., 2008; Marimon-Júnior *et al*., 2019).

Although the occurrence and monodominance of some Neotropical forests are not conditioned by restrictive climatic conditions, differences in the distribution of light and in the species-specific capacities for the use of this resource is one of the factors of most significant repercussion for the structuring such forests (Marimon *et al*., 2008; Peh *et al*., 2011). *B. rubescens* has its development closely related to the amount and quality of irradiation it receives, and to the morphological and anatomical characteristics that provide phenotypic plasticity and periodical growth (Marimon et al. 2001, 2012). Also, soils affect the demography of *B. rubescens* in the different phases of development, and the soil where this species is found has been reported to be poor (Quesada et al. 2010; Marimon-Junior et al. 2019). On the hydric component, some studies have shown that *B. rubescens* invests in greater root biomass under the condition of more solar irradiation as a response to seasonal hydric deficits, but the response of that species to the climatic environmental dynamics is unknown (Marimon et al. 2008, 2012).

The temporal and spatial maintenance of *B. rubescens* monodominant forests is linked to episodic recruitment in response to climatic interference, mainly associated with the impacts of prolonged drought disturbances related to *El Niño* Southern Oscillation phenomenon (ENSO, Marimon et al. 2014, Marimon-Junior et al. 2019). Despite the morpho-anatomical and physiological attributes and environmental adaptations of *B. rubescens*, these drought events have caused a drastic reduction in regeneration, which may contribute to its population decline, monodominant and mixed, in the Amazonia-Cerrado transition (Marimon et al. 2012, 2020). In this sense, future climatic variations may affect the sensitive balance between mortality and recruitment, affecting the local and regional distribution of *B. rubescens*. Despite several studies about the monodominant forest of *B. rubescens*, the patterns of the spatial distribution of this species using different sets of variables and its spatial trends in future climate change scenarios are not yet understood. In this work, we aimed to: 1) determine how

the spatial distribution patterns of *B. rubescens* vary with different environmental predictive variables, and 2) evaluate the temporal and spatial persistence of *B. rubescens* in the Neotropics. Knowing the spatial and temporal patterns of this species would facilitate the planning of management strategies for conservation.

Materials And Methods

Study area

The results of the models were restricted to the northern portion of the South American continent (Fig. 1 and Supplementary Material S2), but to generate the models, the Neotropical region was chosen (Leroy et al. 2018).

B.rubescens is a canopy species belonging to the Moraceae family (Berg 1972) that can reach 90 cm of diameter at breast height with heights of up to 35 m (Laurance et al. 2004). In Brazil, the main biomes where the species is reported are Amazonia, Cerrado, and Atlantic Forest, with spatial interruptions that coincide with the Caatinga Biome and monodominant forests registered only in Amazonia-Cerrado transition zone (Marimon et al. 2014, 2020). The region is characterized by a high spatial interconnection and continuity of the Amazonia Biome associated with an extensive hydrographic network (Wiens and Donoghue 2004; Senior et al. 2019). In Amazonia and Atlantic biomes the soils are dystrophic but shallow for the former and humid and deep for the latter (Quesada et al. 2010; Joly et al. 2012). On the other hand, Cerrado soils are highly weathered and deep, with acidic pH, low fertility, and high levels of iron and aluminum (Ribeiro and Walter 2008).

OCCs: Obtaining and preprocessing

We obtained the occurrence data (OCCs: Fig. 2a) for *B. rubescens* from the virtual platforms GBIF (http://www.gbif.org) and speciesLink (http://splink.cria.org.br), complemented with data from the Laboratório de Ecologia Vegetal (Universidade do Estado de Mato Grosso, Nova Xavantina). We incorporate all OCCs data regardless of the sampling date. The initial database had 256 records that we filtered spatially to identify and eliminate data that were outside the Neotropical region. Subsequently, we eliminated all repeated, null, or dubious taxonomic data.

A common problem in data obtained from virtual platforms is the spatial biases associated with the frequency, intensity and, heterogeneity of the sampling efforts (de Oliveira et al. 2014; De Marco and Nóbrega 2018). Using KDE (Kernel Density Estimation) spatial heterogeneity (Silverman 2018), was evidenced in the OCCs of *B. rubescens* (Fig. 1). To obtain the KDE, at the QGIS software (version 3.14; Quantum GIS Geographic Information System; QGIS.org 2020), we used the interpolation extension ´Heatmap´ with Epanechnikov Kernel function and 10,000 km as bandwidth value. We evaluated the spatial autocorrelation (SAC) of the OCCs using Moran index (Fig. 2a). As the data presented SAC (values greater than |0.2|) and spatial heterogeneity, we applied the “spThin” package with 10 km as the cutoff value (Aiello-Lammens *et al.*, 2015) from the R platform (R Core Team 2020).

Preparation of environmental predictors

To better approximate the fundamental niche of *B. rubescens* we used predictive environmental variables (Supplementary Material S1) known to present an effect at different scales and magnitudes (Soberon 2010).

Environmental variables act with spatial connections that follow a spatial hierarchical dependence pattern, with climate acting on the global scale, geomorphology on the regional scale, and hydrological variables on the local scale (Wiens and Donoghue 2004; Domisch et al. 2015). In this sense, despite the system emergence properties, evaluating each set of variables in blocks (climate, edaphic and hydric) may promote a better understanding of the effect of each set on the spatial patterns (Velazco et al. 2017).

We established three subsets of environmental predictors: climatic, edaphic, and hydric variables. In the climatic subset, we used 19 predictor variables obtained from the WorldClim platform (http://www.worldclim.org, Hijmans et al. 2005). For the edaphic characterization, we used 17 variables (Supplementary Material Fig. 1) obtained from the SoilGrids project (http://www.soildgrids.org).

As described in different studies, life cycles, biomass dynamics, growth, stature, and species distribution are conditioned by the seasonality of climatic variables related to hydric stress (Bruijnzeel 2004; Feldpausch et al. 2011, 2016). In this sense, we incorporated 23 variables in the hydric subset (Supplementary Material Fig. 1) obtained from different platforms: six variables from the Potential EvapoTranspiration (http://www.cgiar-csi.org), one from Actual EvapoTranspiration, and three from Soil Water Stress (http://www.cgiar-csi.org/data), being six variables of Relative Humidity (https://www.climond.org), three of Cloud Cover (http://www.cgiar-csi.org/data), three of Water Vapor Pressure (http://worldclim.org/version2) and one Topographic Wetness Index variable (http://envirem.github.io).

Considering the relative temporal homogeneity and importance for the characterization and physical description of the landscape of the five following variables: Global Relief Model (http://geodata.grid.unep.ch), Elevation, Slope and, Aspect (http://srtm.csi.cgiar.org) and Terrain Roughness Index (http://envirem.github.io), we included them to each one of the three subsets described above.

To generate the Species Distribution Models (SDMs) of past and future projections, we selected three scenarios: Last Glacial Maximum (LGM: 22,000 years ago), Middle Holocene (MH: 6000 years ago), and Future (F: 2041–2060). We also used three models of global circulation for the selected periods: CCSM4, MPI-ESM-P and, MIROC-ESM; these models, from the WorldClim platform, were chosen because they generate robust temporal projections (Hijmans et al. 2005; Carnicer et al. 2020). Due to the increase in greenhouse gas emissions and trends expected for the future (Riahi et al. 2011; IPCC 2013), we considered the most extreme emission scenario [RCPs (Representative Concentration Paths) = 8.5].

We standardized all environmental predictor variables (μ=0.1, SD=1) to avoid different weights (Fig. 2). Subsequently, we adjusted all variables to 10 km of resolution and cropped them using a Neotropical mask. Finally, we established different treatments from the subsets of environmental predictor variables performing PCAs to reduce data collinearity (De Marco and Nóbrega 2018): PCA1 (C: 24 climatic variables), PCA2 (E: 22 edaphic variables), PCA3 (H: 28 hydric variables), PCA4 (CEH-1: all variables together, 69), and the PCAs for the LGM (Last Glacial Maximum), MH (Middle Holocene) and F (FUTURE) scenarios. In each PCA, we retained the first axes that together explained more than 95% of the original environmental variation. We also obtained the independent contributions of each variable considered in the axes of all PCAs (Supplementary Material Fig. 1).

SDM methods configuration and evaluation

We applied the SDMs that present greater predictive performances and flexibility with presence-only data (Fig. 2c), using the following algorithms: BIOCLIM (BIO), GOWER (GWR), MAXENT (ME), Generalized Linear Models (GLM), Random Forest (RF) and Support Vector Machine (SVM).

To meet the requirements of the algorithms, we generated 10,000 background points randomly distributed within the study area, without spatially coinciding with known occurrence points. Then, we divided the data into 70% for test and 30% for training and validation. We generated the first models for the present scenario (PCA1, PCA2, PCA3, and PCA4) and later for the LGM, MH, and F scenarios. To obtain the potential distribution of *B. rubescens,* we used the most straightforward configurations of the models (Varela et al. 2011), leaving the results to depend on the interactions between the algorithms and the input data (Fig. 2d).

We executed and built all SDMs using the R “dismo” package (Hijmans et al. 2015) using the specific functions of each algorithm. With some exceptions, we configured the SVM models from the “ksvm” function of the “kernlab” package (Karatzoglou et al. 2004) and RF from the “randomForest” package (Liaw and Wiener 2002). Moreover, we defined the randomization process to 30 iterations for each algorithm (using a self-initialization analysis) to decrease the spatial structure between the training and test data (subsets of the same OCC points), to reduce possible correlation errors, and to reduce biased evaluations. Thus, we generated 180 models for each set of predictive variables, totaling 1,260 models.

We used as a threshold the lowest adequacy value within the incorporated OCCs (LPT: Lowest Presence Training; Pearson et al. 2007), allowing the generation of presence/absence matrices (binary models) from the adequacy of continuous matrices projected for South America (environmental models). Applying the consensus of the weighted average we assembled all the suitability matrices obtained for the different temporal scenarios. In this way, to generate a final distribution matrix for *B. rubescens* in the temporal scenarios, we applied a consensus method, assembling all the predictions considering only those models with TSS values greater than the mean TSS value.

The performance of the SDMs generated was evaluated by two families of statistical metrics: dependent and independent thresholds (Liu et al. 2005). In this sense, we applied the TSS (True Skill Statistic estimator) (Allouche et al. 2006) in which the response values vary between -1 to 1 where SDMs > 0.5 are considered acceptable or adequate (Allouche et al. 2006). To complement, we applied the independent threshold AUC (Area Under the receiver-operator Curve) (Fielding and Bell 1997), which discriminates areas of omission from areas with known occurrence. Values range from 0 to 1, where the closer to 1 the better is the model's ability to represent reality (Elith 2000). To verify the differences in AUC and TSS values among the PCAs and the applied algorithms we performed Kruskal-Wallis non-parametric tests since the data didn’t meet the assumption of normality.

Results

Model evaluation

All algorithms showed high performance and there were statistical differences among them (Fig. 3). Moreover, all models showed TSS and AUC adequate values (Table 1), but the best performances were associated with the SVM, ME, and RF algorithms, with TSS values > 0.5 and AUC > 0.8 (Table 1, Fig. 3). The models generated exclusively from hydric variables and combining all the variables performed better, regardless of the algorithms (Table. 1). For both PCAs and algorithms, the null hypothesis was rejected (p-value <0.001) (Fig. 3).

Table 1

Mean values of AUC (Area Under the receiver-operator Curve) and TSS (True Skill Statistic) of the different SDMs applied to assess the distribution of *B. rubescens* in the treatment of Climate (C), Edaphic (E), Water (H), Climate + Edaphic + Water (CEH-1) and the Last Glacier Maximum (LGM), Middle Holocene (MH) and Future (F) scenarios.

Algorithms	**C** (PCA1)		**E** (PCA2)		**H** (PCA3)		**CEH-1** (PCA4)		Total (AUC)	Total (TSS)
	AUC	TSS	AUC	TSS	AUC	TSS	AUC	TSS		
BIO	0.741	0.417	0.710	0.359	0.753	0.436	0.757	0.458	0.740	0.417
GLM	0.805	0.566	0.756	0.489	0.797	0.528	0.808	0.598	0.792	0.545
GWR	0.726	0.376	0.715	0.394	0.781	0.504	0.784	0.501	0.752	0.444
ME	0.812	0.560	0.769	0.481	0.810	0.560	0.823	0.620	0.803	0.555
RF	0.832	0.598	0.784	0.458	0.832	0.542	0.837	0.621	0.821**	0.555**
SVM	0.798	0.544	0.768	0.460	0.823	0.557	0.818	0.588	0.801	0.537
Total (PCAs)	0.786	0.510	0.750	0.440	0.799	0.521	0.804*	0.564*	0.785	0.509

*Higher values of AUC and TSS comparing the different sets of variables.

**Higher AUC and TSS values of the different SDMs applied.

Present projections

The spatial complexity of the generated predictions was different depending on the built-in predictor variables. The suitability matrices generated from PCA1 (C: climatic variables) and PCA3 (H: hydric variables) showed greater continuity and spatial aggregation (Fig. 4). The matrices generated from the PCA3 (E: edaphic variables) showed diffuse spatial patterns of greater amplitude and spatial complexity (Fig. 4). When considering all the variables together (CEH-1), two situations can be observed: high connectivity in spatial patterns and/or low spatial complexity concerning the other PCAs used. Regardless of the variables incorporated, all models showed centers of greater suitability in the central region of the Amazon Basin, the Atlantic coast, and the North region of South America (Fig. 4). As a particular case, CEH-1 showed predictions of suitability associated with the Central America and the Caribbean islands, although we have not incorporated

occurrence records for these areas. Regardless of the set of built-in predictor variables, the predictions of environmental suitability were superimposed on the occurrence records obtained in the field.

When we combined all the variables to assess the independent contribution of each within a 200,000 km^2 hexagon, we observed in more detail the environmental structure (climatic, edaphic and hydric) of the study area (CEH-2, Fig. 4). In this sense, in the Amazon Basin and Atlantic coast, the balance between the three sets of variables makes it possible to recognize the higher values of environmental suitability.

Projections of temporal climate scenarios

The spatial patterns of the models for different scenarios showed some overlap in the historical spatial patterns of *B. rubescens* (Fig. 5). Despite the "temporal distance" of the compared scenarios, the environmental suitability matrices (Fig. 5: Species model distribution) show high spatial overlap, with good connectivity, being more significant and evident in the environmental suitability centers that are associated with the Amazon Basin, North of South America and Atlantic coast.

Although the matrices obtained from the projections have diffuse regions, both for the past scenarios (LGM and MH) and the future (F), the highest suitability values are superimposed on the present spatial patterns (CEH-1). The projections were made using only climatic variables and not considered them as predictors of the landscape, such as topographic or edaphic variables.

While we did not incorporate occurrence records for Central America or the Caribbean island system, projections for both past and future scenarios showed environmental suitability associated with these regions. The suitability matrices for all temporal projection scenarios also show values associated with the Patagonian region, with greater spatial amplitude of predictions in the LGM and F scenarios. On the other hand, in the matrices of all projections two large areas can be seen, one between the Caribbean coasts and Amazonia and the other between the Amazonia biome and the Atlantic Forest.

The pattern of spatial overlap between different scenarios can be highlighted in higher resolution in the binary matrices (Fig. 5: Binary models). The PPF (Present Past and Future) map is the result of overlapping all of them in a single matrix (Fig. 5). The values associated with each binary matrix represent the amount of area (km^2) that *B. rubescens* occupies within the study area. The central triangle shows surface losses and gains from one scenario to another. A surface gain of 932,659 km^2 can be noticed from the LGM to the CEH-1 (present). Also, it shows a substantial loss from the present to the future projection of 568,118 km^2. However, this loss is not total: when comparing the surface calculated for the LGM with the amount of surface that was projected for the future, the result remains positive (Fig. 5). Despite these variations in the total surface values over time, in the PPF matrix, it can be seen that *B. rubescens* has a high and recurring presence associated with the coastal region of the South American Caribbean, Amazon Basin, and the Atlantic forest, where we found highest adequacy values for all projections made (Fig. 5).

Discussion

The spatial patterns predicted for *B. rubescens*, regardless of the variables, allowed a great spatial and historical description of the potential niches of the species in the Neotropical region. All algorithms showed high performance, with greater responses for water variables and all predictors combined. The spatial patterns predicted using edaphic variables showed higher complexity, amplitude, and spatial connectivity than those predicted in a similar way for climatic and, water variables, which suggests that the potential niches of *B. rubescens* can be defined by climatic fluctuations, with the edaphic conditions being non-restrictive of their presence in the evaluated spatial scale. Yet, historical patterns showed high spatial overlap and geographic fidelity, with increases in spatial amplitude from the past to the present and decrease from the present to the future.

Brosimum rubescens and climate

The SDMs predictions obtained from climatic variables showed high performance, strong relationship, and dependence between climate and the spatial distributions of the vegetation. Results supported and found in multiples works of vegetation SDM with climatic variables. (Peh et al. 2011; Velazco et al. 2017; Soong et al. 2020). The models showed suitable areas highly connected and spatially continuous, however, with two spatial segregations, one in the Amazonia biome and the other associated with the Atlantic Forest. Climatic conditions are very similar in the central region of Amazonia and the Hiléia Baiana within the Atlantic Forest in Brazil (Andrade-Lima 1966; Gentry 1982; Sobral-Souza et al. 2015). Following the Köppen-Geiger (Beck et al. 2018) climate classification, these two regions share similar climatic conditions, corresponding to climatic zones Af (equatorial), Am (monsoon), and Aw (savanna). Mainly Af and Am are characterized by being tropical and without a dry season (or short dry season), in fact, the low prediction associated with the Amazonia-Cerrado transition (Aw type) corresponds to a tropical climate with a more extended dry season (Beck et al. 2018).

Topographic variables GRM (Global Relief Model) and Elevation were also selected within PCA1, these variables, together with pluviometry, condition the temporal and spatial connectivity of hydrological networks (Marimon-Junior 2007; Domisch et al. 2015; Parreira et al. 2019). For some monodominant species, precipitation is important due to its impacts on water table fluctuations and flood pulses (Nunes Da Cunha and Junk 2001). For *B. rubescens,* fruiting and seed dispersal processes are associated with the beginning of the rainy season (Rivera et al. 2014). Also, ENSO-related extreme drought events affect negatively the recruitment and survival rates of this species. (Laurance 2003; Phillips et al. 2010; Marimon et al. 2020). *B. rubescens* is a light-demanding species with episodic recruitment and depends on the temporal variations of light and temperature (Marimon et al. 2012). Although variables that could characterize this dynamic were not incorporated into our analysis, some variables such as those of cloud cover could act as proxies for this spatial variation of the environment (Clark and Clark 1994).

Brosimum rubescens and edaphic variables

Edaphic properties have been considered the best predictors of wood species spatial distribution (Velazco et al. 2017; Elias et al. 2018). Nevertheless, our edaphic variables models, though showing high performance didn’t obtain the highest values of AUC and TSS. The spatial patterns of suitability predictions obtained from the edaphic variables had greater amplitude and spatial complexity than the other variables, with a strong

association with the Amazonia central region and the Atlantic coast. The Amazonia region and Atlantic coast have similar edaphic conditions, with deep soils, predominantly Oxisols, and Argisols (Quesada et al. 2010; Marimon-Junior et al. 2019).

B. rubescens is considered an accumulator of manganese and aluminium; this, and its association with soils rich in potassium, may favor its reproductive success and dominance (Elias et al. 2018). Some forests with high abundance of *B. rubescens* also reportedly have high Mg/Ca ratios; however, it is unclear whether this factor is related to the species distribution and dominance (Marimon et al. 2001; Marimon-Junior 2007). Even so, high concentrations of exchangeable cations in the soil could act as a competitive advantage allowing the species to have a wide range of niches (Elias et al. 2019; Marimon-Junior et al. 2019), as observed in the models obtained from edaphic variables. Moreover, some studies suggest that edaphic properties affect *B. rubescens* according to the ontogenetic stage, thus the dependency relationship of this species with the edaphic properties increases in complexity (Brito-Rocha et al. 2016; Elias et al. 2018).

Brosimum rubescens and hydric variables

The spatial distributions of the predictions of suitability generated from hydric variables showed high spatial connectivity, few diffuse areas, and spatial overlap with the Amazonas-Tocantins-Araguaia hydrographic networks and the East Atlantic and East-Northeast Atlantic Basins. Water environmental predictors are primarily responsible for defining vegetation hydric conditions (Borchert 1994; Anderegg et al. 2018; Bittencourt et al. 2020). Fluctuations in hydric properties act as a strong environmental filter, spatially segregating phytophysiognomies according to hydric stress tolerance thresholds (Borchert 1994; Bittencourt et al. 2020). In the geographical extension (Leroy et al. 2018) delimited in our case, the Neotropics, the climate and the edaphic properties may affect the predictions on macro-ecological spatial scales (regional or continental) and the water variables could be acting on smaller spatial scales (Domisch et al. 2015; Velazco et al. 2017).

We observed that soil water stress (SWS) and topographic humidity index (TWI) were related to *B. rubescens* occurrence. Drought is an important factor related to the hyperdynamisms of tropical forests, affecting the structure, dynamics, and composition of tree species (Marimon et al. 2012). The regeneration of this species may be conditioned by decreases in the availability of water derived from droughts during and after ENSO events (Marimon et al. 2020). However, *B. rubescens* also produce larger amounts of seeds during drought periods (Marimon and Felfili 2006), and this strategy may be advantageous for maintaining its dominance (Rivera et al. 2014).

Brosimum rubescens and CEH-1

Each set of variables can generate different predictions for a species, but the combination of all these variables in a single subset allows a better representation of ecosystems by improving the approximations of the fundamental niche (Velazco et al. 2017). When the different subsets of variables were combined in a single block (CEH-1), the result for *B. rubescens* showed a balance in the values of AUC and TSS (De Marco and Nóbrega 2018). When the variables are incorporated into subsets, they respond at their thresholds, but when

they are complemented, they respond with spatial hierarchical dependence (Rivera et al. 2014; Domisch et al. 2015; Elias et al. 2018).

The environmental suitability matrices obtained from the CEH-1 scenario were adjusted to the spatial patterns of occurrence reported for *B. rubescens* within the study area. The spatial distribution pattern of the Brosimeae tribe extends from Mexico to southern Brazil, with records in some Antilles islands (Cuba and Jamaica) and many species associated with the Amazon Basin (Berg 1972). In the Neotropics, *B. rubescens* are spatially discontinuous, but the highest frequency of records is associated with the Amazon Basin in Brazil, Peru, Colombia, and Guianas (Berg 1972). In the Brazilian Amazonia-Cerrado transition, *B. rubescens* form extensive monodominant forests (Marimon et al. 2001, 2020). In central Amazonia, this species had greater spatial connectivity in the environmental suitability.

As evidenced in the CEH-2 map, the regions where the balance between climatic, edaphic, and hydraulic factors was greater for this species had a high spatial overlap with the matrices of environmental suitability obtained with the different algorithms. Other areas where the proportions of C, E, and H, were not in balance, showed the possible limiting factors for the absence. An example of this would be the region of Patagonia where environmental suitability was predicted, but it would only be the edaphic variables (and climate in a smaller proportion) that would facilitate the presence of *B. rubescens* in this region, as the hydric conditions do not allow its development.

Brosimum rubescens and historical occurrence

In our results, we observed variation in the spatial amplitudes of the environmental suitability projected in the different temporal scenarios. Other studies have suggested that decreases in population densities over time in conjunction with the predominantly random spatial pattern may be responding to density-dependent mortality (Felfili et al. 2000; Arieira et al. 2016), so when evaluating different dominant species of tropical forests, we can conclude that those with lower spatial densities tend to disappear more easily. After recent drought events, *B. rubescens* showed variations in population density and demography, mainly in the regenerating stratum, but the robustness of the intraspecific spatial pattern was maintained for the trees, demonstrating resistance and resilience of the species to exogenous disturbances (Elias et al. 2018; Marimon et al. 2020). In this sense, the extreme climate events may not change the spatial pattern of the Neotropical distribution of *B. rubescens*, as was observed on a smaller spatial scale by (Elias et al. 2018). However, according to the silvigenetic cycle, *B. rubescens* may be emerging from a possible post-disturbance phase in the construction cycle (Hallé et al. 1978; Elias et al. 2018), suggesting that anthropic disturbances and clearing openings may have greater weight in their demographic and spatial patterns.

It is unknown whether, at present, *B. rubescens* is in successional or climax stages, and if future climatic changes will affect the balance between mortality and recruitment of this species. Increases in mortality can reduce intraspecific competition and increase the spatial aggregation of this species (Elias et al. 2018), and this pattern, on a larger spatial scale, was observed in our study in the transition from CURRENT-FUTURE environmental suitability projections. Moreover, the reverse demographic pattern (decrease in mortality and increases in recruitment), could be a result of the diffuse and disaggregated spatial pattern in the transition of the UMG-CURRENT scenarios.

Following the BAM diagram (Soberon 2010), our models did not consider the bionomic factors, which may have masked some effects of unknown magnitude on the distribution patterns of *B. rubescens* in space and time (Rivera et al. 2014). For example, our model didn't account for positive associations with species from different strata or local competitive exclusion (Elias et al. 2018) and, by extension, the representation of spatial dynamics and heterogeneity of environments where the species occurs. However, the strategies for spatial occupation and temporal maintenance of the occurrence areas are well characterized in the SDMs (Marimon et al. 2001; Soberon 2010; Elias et al. 2018).

Conclusion

Our results show the independent and combined effects of different environmental variables, allowing us to identify what limit or facilitate the spatial distribution of B. rubescens in the Neotropics. At the same time, we corroborate the spatial persistence and geographic fidelity of the spatial patterns of the species over time. In SDMs, the climatic predictors can define the distribution patterns, however, the edaphic conditions can be restrictive. In our case, B. rubescens has a wide spatial distribution if we consider the edaphic configuration and a more restricted distribution if we consider climatic or hydric predictors. Knowing the responses of species to environmental variables that condition their spatial and historical patterns are results of high impact in the global context of human actions and intensification of climate change.

Declarations

FUNDING

This study was financed in part by the *Coordenacão de Aperfeiçoamento de Pessoal de Nível Superior*-Brazil (CAPES) - Finance Code 001. We also thank the *Conselho Nacional de Desenvolvimento Científico e Tecnológico/Projetos Ecológicos de Longa Duração-CNPq/PELD* (Nr. 441244/2016-5), for financial support. B.S. Marimon and B.H. Marimon-Junior acknowledge CNPq for their productivity grants (305029/2015-0 and 301153/2018-3), and P.S. Morandi acknowledges CAPES for his post-doc grant (88887.185186/2018-00). T.R. Feldpausch was supported by the UK Natural Environment Research Council (NERC, NE/N011570/1).

CONFLICTS OF INTEREST/COMPETING INTERESTS

The authors declare they have no conflict of interests to declare.

ETHICS APPROVAL

Not applicable.

CONSENT TO PARTICIPATE

Not applicable.

CONSENT FOR PUBLICATION

All authors agree to the publication the present work.

VAILABILITY OF DATA AND MATERIAL

Species occurrences are available in the supplementary material.

CODE AVAILABILITY

Available upon request.

AUTHORS' CONTRIBUTIONS

Conceived and designed the investigation: FA, PSM, BHM-J, RE, IA, LHM, AOM, BSM. Performed field and laboratory work: FA, PSM, IA, LHM, AOM. Analyzed the data: FA, RE. Contributed materials and analysis tools: FA, RE, BHM-J, TRF, BSM. Wrote the paper: FA, PSM, BHM-J, RE, IA, LHM, AOM, TRF, BSM.

References

1. Aiello-Lammens ME, Boria RA, Radosavljevic A, et al (2015) spThin: An R package for spatial thinning of species occurrence records for use in ecological niche models. Ecography (Cop) 38:541–545. https://doi.org/10.1111/ecog.01132
2. Allouche O, Tsoar A, Kadmon R (2006) Assessing the accuracy of species distribution models: Prevalence, kappa and the true skill statistic (TSS). J Appl Ecol 43:1223–1232. https://doi.org/10.1111/j.1365-2664.2006.01214.x
3. Anderegg WRL, Konings AG, Trugman AT, et al (2018) Hydraulic diversity of forests regulates ecosystem resilience during drought. Nature 561:538–541. https://doi.org/10.1038/s41586-018-0539-7
4. Andrade-Lima AD (1966) Contribuição ao estudo do paralelismo da flora Amazônico-Nordestina, 1st edn. Secretaria de Agricultura, Indústria e Comércio, Recife
5. Arieira J, Penha J, Nunes da Cunha C, Couto EG (2016) Ontogenetic shifts in habitat-association of tree species in a neotropical wetland. Plant Soil 404:219–236. https://doi.org/10.1007/s11104-016-2844-y
6. Beck HE, Zimmermann NE, McVicar TR, et al (2018) Present and future köppen-geiger climate classification maps at 1-km resolution. Sci Data 5:180214. https://doi.org/10.1038/sdata.2018.214
7. Berg CC (1972) Flora Neotropica - Monograph No. 7: Olmedieae, Brosimeae (moraceae), Reprinted. Hafner Publishing Company, Inc, New York
8. Bittencourt PRL, Oliveira RS, da Costa ACL, et al (2020) Amazonia trees have limited capacity to acclimate plant hydraulic properties in response to long-term drought. Glob Chang Biol 26:3569–3584. https://doi.org/10.1111/gcb.15040

9. Borchert R (1994) Soil and Stem Water Storage Determine Phenology and Distribution of Tropical Dry Forest Trees. Ecology 75:1437–1449. https://doi.org/10.2307/1937467
10. Brito-Rocha E, Schilling AC, Dos Anjos L, et al (2016) Regression models for estimating leaf area of seedlings and adult individuals of Neotropical rainforest tree species. Brazilian J Biol 76:983–989. https://doi.org/10.1590/1519-6984.05515
11. Bruijnzeel LA (2004) Hydrological functions of tropical forests: Not seeing the soil for the trees? Agric Ecosyst Environ 104:185–228. https://doi.org/10.1016/j.agee.2004.01.015
12. Carnicer C, Eisenlohr P V., Jácomo AT de A, et al (2020) Running to the mountains: mammal species will find potentially suitable areas on the Andes. Biodivers Conserv 29:1855–1869. https://doi.org/10.1007/s10531-020-01951-5
13. Clark DA, Clark DB (1994) Climate-Induced Annual Variation in Canopy Tree Growth in a Costa Rican Tropical Rain Forest. J Ecol 82:865. https://doi.org/10.2307/2261450
14. De Marco P, Nóbrega CC (2018) Evaluating collinearity effects on species distribution models: An approach based on virtual species simulation. PLoS One 13:202403. https://doi.org/10.1371/journal.pone.0202403
15. de Oliveira G, Rangel TF, Lima-Ribeiro MS, et al (2014) Evaluating, partitioning, and mapping the spatial autocorrelation component in ecological niche modeling: A new approach based on environmentally equidistant records. Ecography (Cop) 37:637–647. https://doi.org/10.1111/j.1600-0587.2013.00564.x
16. Domisch S, Jähnig SC, Simaika JP, et al (2015) Application of species distribution models in stream ecosystems: The challenges of spatial and temporal scale, environmental predictors and species occurrence data. Fundam Appl Limnol 186:45–61. https://doi.org/10.1127/fal/2015/0627
17. Elias F, Marimon BS, Marimon-Junior BH, et al (2018) Idiosyncratic soil-tree species associations and their relationships with drought in a monodominant Amazon forest. Acta Oecologica 91:127–136. https://doi.org/10.1016/j.actao.2018.07.004
18. Elias F, Marimon Junior BH, de Oliveira FJM, et al (2019) Soil and topographic variation as a key factor driving the distribution of tree flora in the Amazonia/Cerrado transition. Acta Oecologica 100:103467. https://doi.org/10.1016/j.actao.2019.103467
19. Elith J (2000) Quantitative methods for Modelling species habitat: comparative performance and an application to Australian plants. In: Ferson S, Burgman M (eds) Quantitative Methods for Conservation Biology, 1st edn. Springer, New York, pp 39–58
20. Feldpausch TR, Banin L, Phillips OL, et al (2011) Height-diameter allometry of tropical forest trees. Biogeosciences 8:1081–1106. https://doi.org/10.5194/bg-8-1081-2011
21. Feldpausch TR, Phillips OL, Brienen RJWW, et al (2016) Amazon forest response to repeated droughts. Global Biogeochem Cycles 30:964–982. https://doi.org/10.1002/2015GB005133
22. Felfili JM, Rezende A V., Da Silva J, Silva MA (2000) Changes in the floristic composition of cerrado sensu stricto in Brazil over a nine-year period. J Trop Ecol 16:579–590. https://doi.org/10.1017/S0266467400001589
23. Fielding AH, Bell JF (1997) A review of methods for the assessment of prediction errors in conservation presence/absence models. Environ Conserv 24:38–49. https://doi.org/10.1017/S0376892997000088
24. Gentry AH (1982) Neotropical floristic diversity: phytogeographical connections between Central and South America, Pleistocene climatic fluctuations, or an accident of the Andean orogeny? Ann - Missouri Bot Gard

69:557–593. https://doi.org/10.2307/2399084

25. Hallé F, Oldeman RAA, Tomlinson PB (1978) Tropical Trees and Forests, 1st edn. Springer Berlin Heidelberg, Berlin, Heidelberg
26. Hart TB, Hart JA, Murphy PG (1989) Monodominant and species-rich forests of the humid tropics: causes for their co-occurrence. Am Nat 133:613–633. https://doi.org/10.1086/284941
27. Hijmans R, Phillips S, Leathwick J, Elith J. (2015) dismo: species distribution modeling. R package
28. Hijmans RJ, Cameron SE, Parra JL, et al (2005) Very high resolution interpolated climate surfaces for global land areas. Int J Climatol 25:1965–1978. https://doi.org/10.1002/joc.1276
29. IPCC (2013) Summary for Policymakers. In: StockerT.F., D. Qin G-K, Plattner MT, et al. (eds) Climate Change 2013: The Physical Science Basis. Contribution of Working Group I to the Fifth Assessment Report of the Intergovernmental Panel on Climate Change. Cambridge University Press, Cambridge, pp 3–29
30. Joly CA, Assis MA, Bernacci LC, et al (2012) Florística e fitossociologia em parcelas permanentes da Mata Atlântica do sudeste do Brasil ao longo de um gradiente altitudinal. Biota Neotrop 12:123–145. https://doi.org/10.1590/s1676-06032012000100012
31. Karatzoglou A, Hornik K, Smola A, Zeileis A (2004) kernlab - An S4 package for kernel methods in R. J Stat Softw 11:1–20. https://doi.org/10.18637/jss.v011.i09
32. Laurance WF (2003) Slow burn: The insidious effects of surface fires on tropical forests. Trends Ecol Evol 18:209–212. https://doi.org/10.1016/S0169-5347(03)00064-8
33. Laurance WF, Nascimento HEM, Laurance SG, et al (2004) Inferred longevity of Amazonian rainforest trees based on a long-term demographic study. For Ecol Manage 190:131–143. https://doi.org/10.1016/j.foreco.2003.09.011
34. Leroy B, Delsol R, Hugueny B, et al (2018) Without quality presence-absence data, discrimination metrics such as TSS can be misleading measures of model performance. J Biogeogr 45:1994–2002. https://doi.org/10.1111/jbi.13402
35. Liaw A, Wiener M (2002) Classification and Regression by randomForest. R News 2:18–22
36. Liu C, Berry PM, Dawson TP, Pearson RG (2005) Selecting thresholds of occurrence in the prediction of species distributions. Ecography (Cop) 28:385–393. https://doi.org/10.1111/j.0906-7590.2005.03957.x
37. Marimon-Junior BH (2007) Relação entre diversidade arbórea e aspectos do ciclo biogeoquímico de uma floresta monodominante de Brosimum rubescens Taub. e uma floresta mista no leste Mato-Grossense
38. Marimon-Junior BH, Hay JDV, Oliveras I, et al (2019) Soil water-holding capacity and monodominance in Southern Amazon tropical forests. Plant Soil 450:65–79. https://doi.org/10.1007/s11104-019-04257-w
39. Marimon BS, Felfili JM (2006) Chuva de sementes em uma floresta monodominante de Brosimum rubescens Taub. e em uma floresta mista adjacente no Vale do Araguaia, MT, Brasil. Acta Bot Brasilica 20:423–432. https://doi.org/10.1590/S0102-33062006000200017
40. Marimon BS, Felfili JM, Fagg CW, et al (2012) Monodominance in a forest of Brosimum rubescens Taub. (Moraceae): Structure and dynamics of natural regeneration. Acta Oecologica 43:134–139. https://doi.org/10.1016/j.actao.2012.07.001
41. Marimon BS, Felfili JM, Haridasan M (2001) Studies in monodominant forests in Eastern Mato Grosso, Brazil: I. a Forest of brosimum rubescens taub. Edinburgh J Bot 58:123–137.

https://doi.org/10.1017/S096042860100049X

42. Marimon BS, Felfili JM, Marimon BH, et al (2014) Leaf herbivory and monodominance in a Cerrado–Amazonia transitional forest, Mato Grosso, Brazil. Plant Biosyst - An Int J Deal with all Asp Plant Biol 150:124–130. https://doi.org/10.1080/11263504.2014.983577
43. Marimon BS, Felfili JM, Marimon Júnior BH, et al (2008) Desenvolvimento inicial e partição de biomassa de Brosimum rubescens Taub. (Moraceae) sob diferentes níveis de sombreamento. Acta Bot Brasilica 22:941–953. https://doi.org/10.1590/s0102-33062008000400005
44. Marimon BS, Oliveira-Santos C, Marimon-Junior BH, et al (2020) Drought generates large, long-term changes in tree and liana regeneration in a monodominant Amazon forest. Plant Ecol 221:733–747. https://doi.org/10.1007/s11258-020-01047-8
45. Murphy BP, Bowman DMJS (2012) What controls the distribution of tropical forest and savanna? Ecol Lett 15:748–758. https://doi.org/10.1111/j.1461-0248.2012.01771.x
46. Nunes Da Cunha C, Junk WJ (2001) Distribution of Woody plant communities along the flood gradient in the Pantanal of Poconé, Mato Grosso, Brazil. Int J Ecol Environ Sci 27:63–70
47. Palacios PA (2005) Patrones estructurales y distribución espacial de poblaciones de Brosimum rubescens taub. En relación con la variabilidad fisiográfica en la ribera colombiana del río amazonas. Universidad Nacional de Colombia-Sede Amazonia
48. Parreira MR, Nabout JC, Tessarolo G, et al (2019) Disentangling uncertainties from niche modeling in freshwater ecosystems. Ecol Modell 391:1–8. https://doi.org/10.1016/j.ecolmodel.2018.10.024
49. Pearson RG, Raxworthy CJ, Nakamura M, Townsend Peterson A (2007) Predicting species distributions from small numbers of occurrence records: A test case using cryptic geckos in Madagascar. J Biogeogr 34:102–117. https://doi.org/10.1111/j.1365-2699.2006.01594.x
50. Peh KSH, Lewis SL, Lloyd J (2011) Mechanisms of monodominance in diverse tropical tree-dominated systems. J Ecol 99:891–898. https://doi.org/10.1111/j.1365-2745.2011.01827.x
51. Phillips OL, van der Heijden G, Lewis SL, et al (2010) Drought-mortality relationships for tropical forests. New Phytol 187:631–646. https://doi.org/10.1111/j.1469-8137.2010.03359.x
52. QGIS.org (2020) QGIS Geographic Information System. Open Source Geospatial Foundation Project. http://qgis.org.
53. Quesada CA, Lloyd J, Schwarz M, et al (2010) Variations in chemical and physical properties of Amazon forest soils in relation to their genesis. Biogeosciences 7:1515–1541. https://doi.org/10.5194/bg-7-1515-2010
54. R Core Team (2020) R: A language and environment for statistical computing. R Foundation for Statistical Computing, Vienna, Austria. ISBN 3-900051-07- 0. http://www.R-project.org/.
55. Riahi K, Rao S, Krey V, et al (2011) RCP 8.5-A scenario of comparatively high greenhouse gas emissions. Clim Change 109:33–57. https://doi.org/10.1007/s10584-011-0149-y
56. Ribeiro JF, Walter BMT (2008) As principais fitofisionomias do bioma Cerrado. In: Sano SM, Almeida SP de, Ribeiro JF (eds) Cerrado: Ecologia e flora, 1st edn. Embrapa Cerrados/Embrapa Informação Tecnológica, Brazil, pp 152–212
57. Rivera LE, Peãuela MC, Moreno F (2014) Intra annual seed production and availability of two morphotypes of Brosimum rubescens taubert in forests of the Colombian Amazon. Biota Neotrop 14:e20130073.

https://doi.org/10.1590/1676-06032014007313

58. Senior RA, Hill JK, Edwards DP (2019) Global loss of climate connectivity in tropical forests. Nat Clim Chang 9:623–626. https://doi.org/10.1038/s41558-019-0529-2
59. Silverman BW (2018) Density estimation: For statistics and data analysis, 1st edn. Routledge, New York
60. Soberon JM (2010) Niche and area of distribution modeling: A population ecology perspective. Ecography (Cop) 33:159–167. https://doi.org/10.1111/j.1600-0587.2009.06074.x
61. Sobral-Souza T, Lima-Ribeiro MS, Solferini VN (2015) Biogeography of Neotropical Rainforests: past connections between Amazon and Atlantic Forest detected by ecological niche modeling. Evol Ecol 29:643–655. https://doi.org/10.1007/s10682-015-9780-9
62. Soong JL, Janssens IA, Grau O, et al (2020) Soil properties explain tree growth and mortality, but not biomass, across phosphorus-depleted tropical forests. Sci Rep 10:1–13. https://doi.org/10.1038/s41598-020-58913-8
63. ter Steege H, Henkel TW, Helal N, et al (2019) Rarity of monodominance in hyperdiverse Amazonian forests. Sci Rep 9:13822. https://doi.org/10.1038/s41598-019-50323-9
64. Torti SD, Coley PD, Kursar TA (2001) Causes and consequences of monodominance in tropical lowland forests. Am Nat 157:141–153. https://doi.org/10.1086/318629
65. Varela S, Lobo JM, Hortal J (2011) Using species distribution models in paleobiogeography: A matter of data, predictors and concepts. Palaeogeogr Palaeoclimatol Palaeoecol 310:451–463. https://doi.org/10.1016/j.palaeo.2011.07.021
66. Velazco SJE, Galvão F, Villalobos F, De Marco P (2017) Using worldwide edaphic data to model plant species niches: An assessment at a continental extent. PLoS One 12:1–24. https://doi.org/10.1371/journal.pone.0186025
67. Wiens JJ, Donoghue MJ (2004) Historical biogeography, ecology and species richness. Trends Ecol Evol 19:639–644. https://doi.org/10.1016/j.tree.2004.09.011

Figures

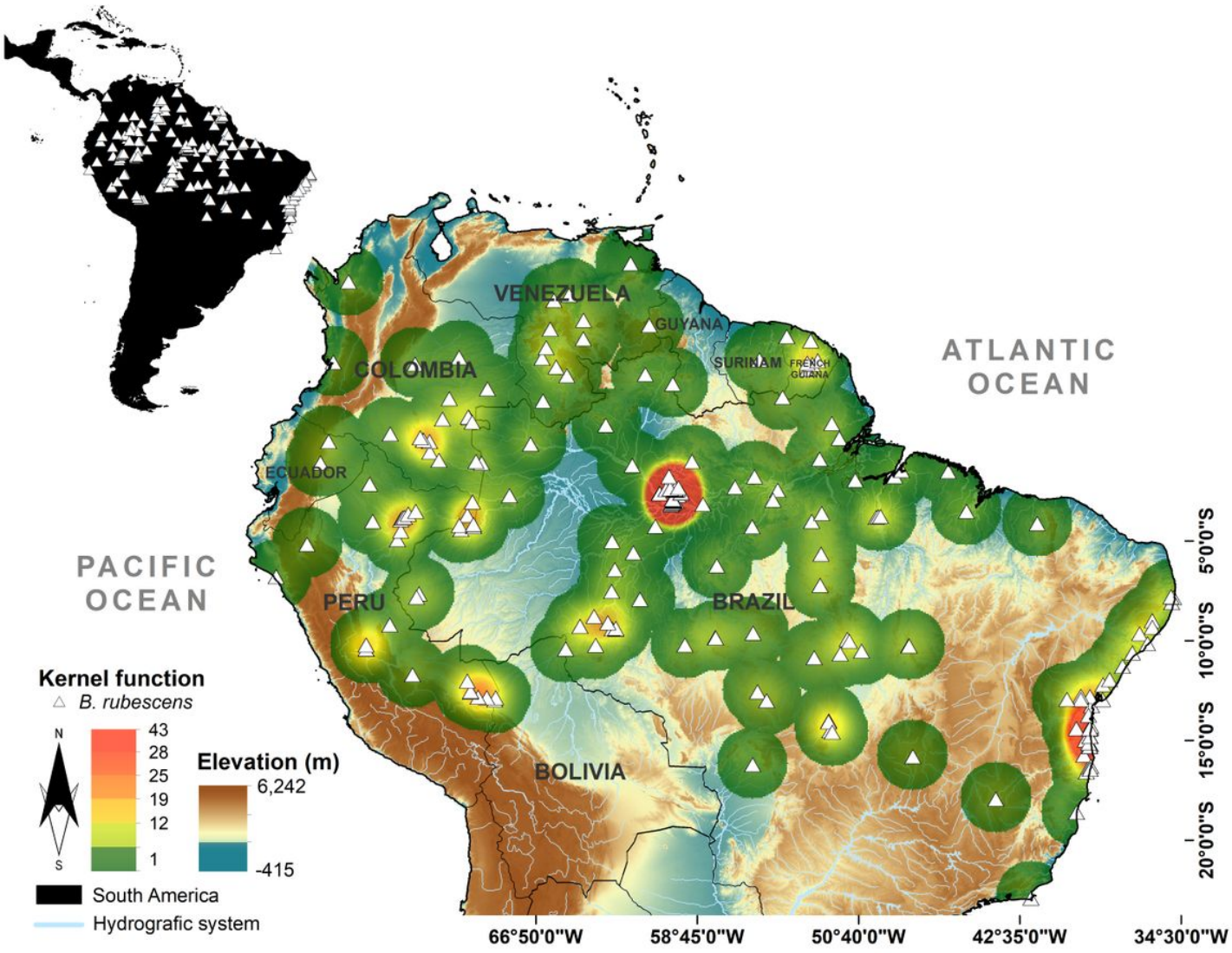

Figure 1

Geographic distribution of spatial records and kernel density estimation (KDE) of B. rubescens in tropical South America, with higher values of density (red) associated with zones with higher frequency and intensity of collection Note: The designations employed and the presentation of the material on this map do not imply the expression of any opinion whatsoever on the part of Research Square concerning the legal status of any country, territory, city or area or of its authorities, or concerning the delimitation of its frontiers or boundaries. This map has been provided by the authors.

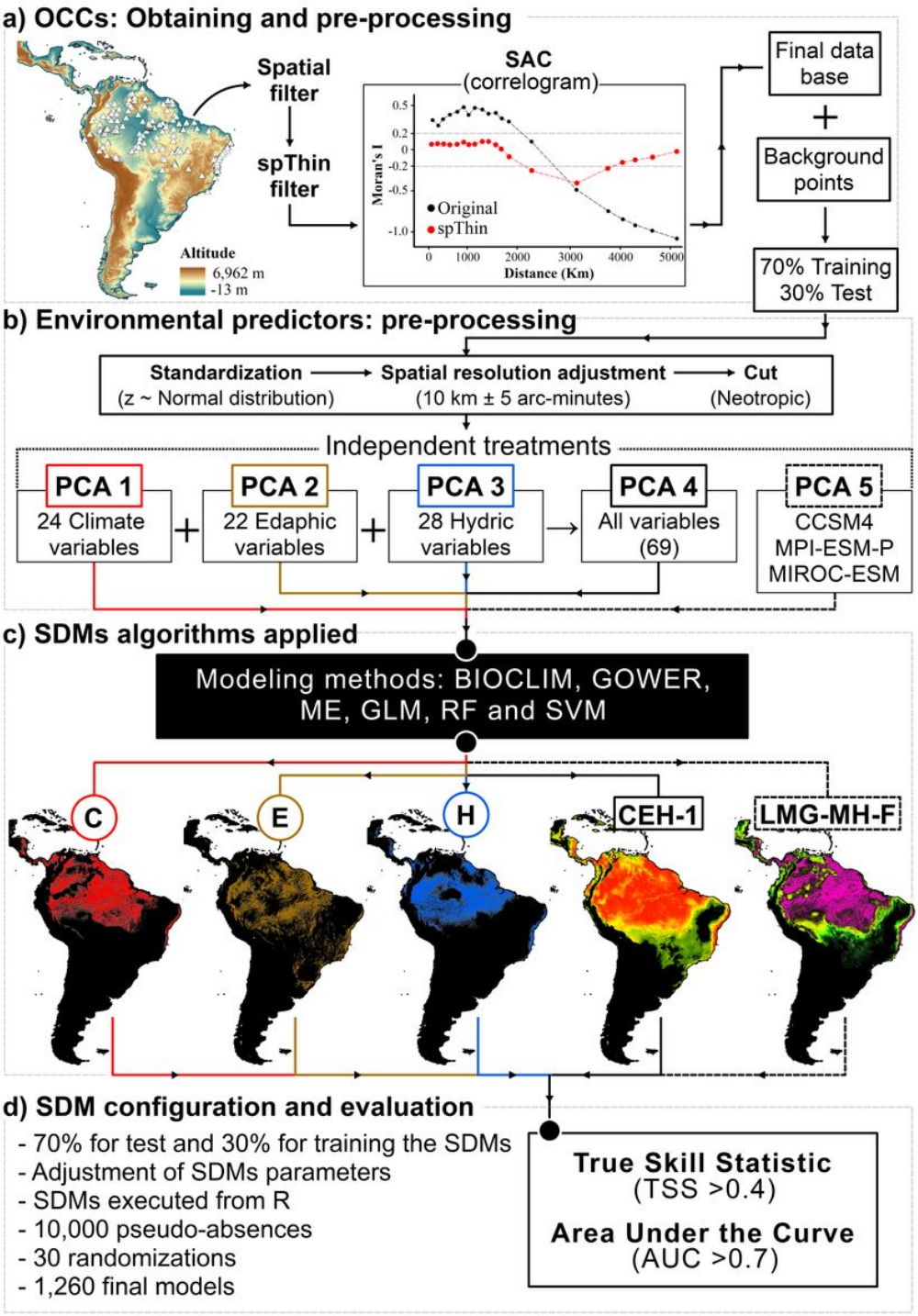

Figure 2

Methodological procedure to obtain SDMs of B. rubescens used Climatic (C), Edaphic (E), Hydric (H), and all combined variables (CEH-1) in the present, Last Glacial Maximum (LGM), Middle Holocene (HM) and future (F) scenarios. The main points are OCCs: Obtaining and pre-processing (A), Preparation of environmental predictors (B), SDM methods applied (C), and SDM configuration and evaluation (D) Note: The designations employed and the presentation of the material on this map do not imply the expression of any opinion whatsoever on the part of Research Square concerning the legal status of any country, territory, city or area or of

its authorities, or concerning the delimitation of its frontiers or boundaries. This map has been provided by the authors.

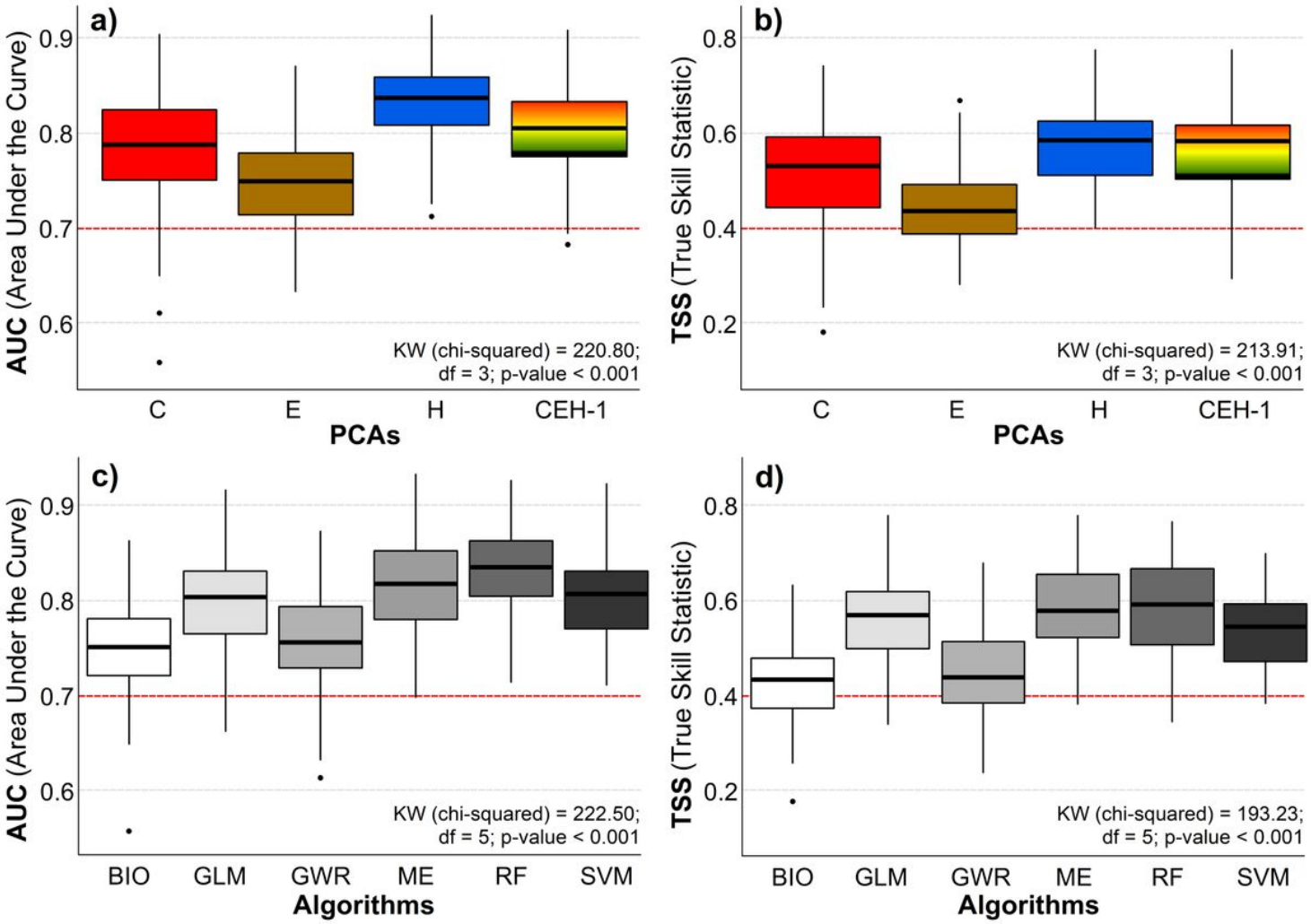

Figure 3

Kruskal-Wallis (KW) distributions of means and standard deviation of AUC and TSS values between different environmental scenarios (Climate: C; Edaphic: E; Hydric: H and CEH-1: all in one) and SDM algorithms (BIO, GLM, GWR, ME, RF and, SVM). The red lines indicate the values from which the models have high performance

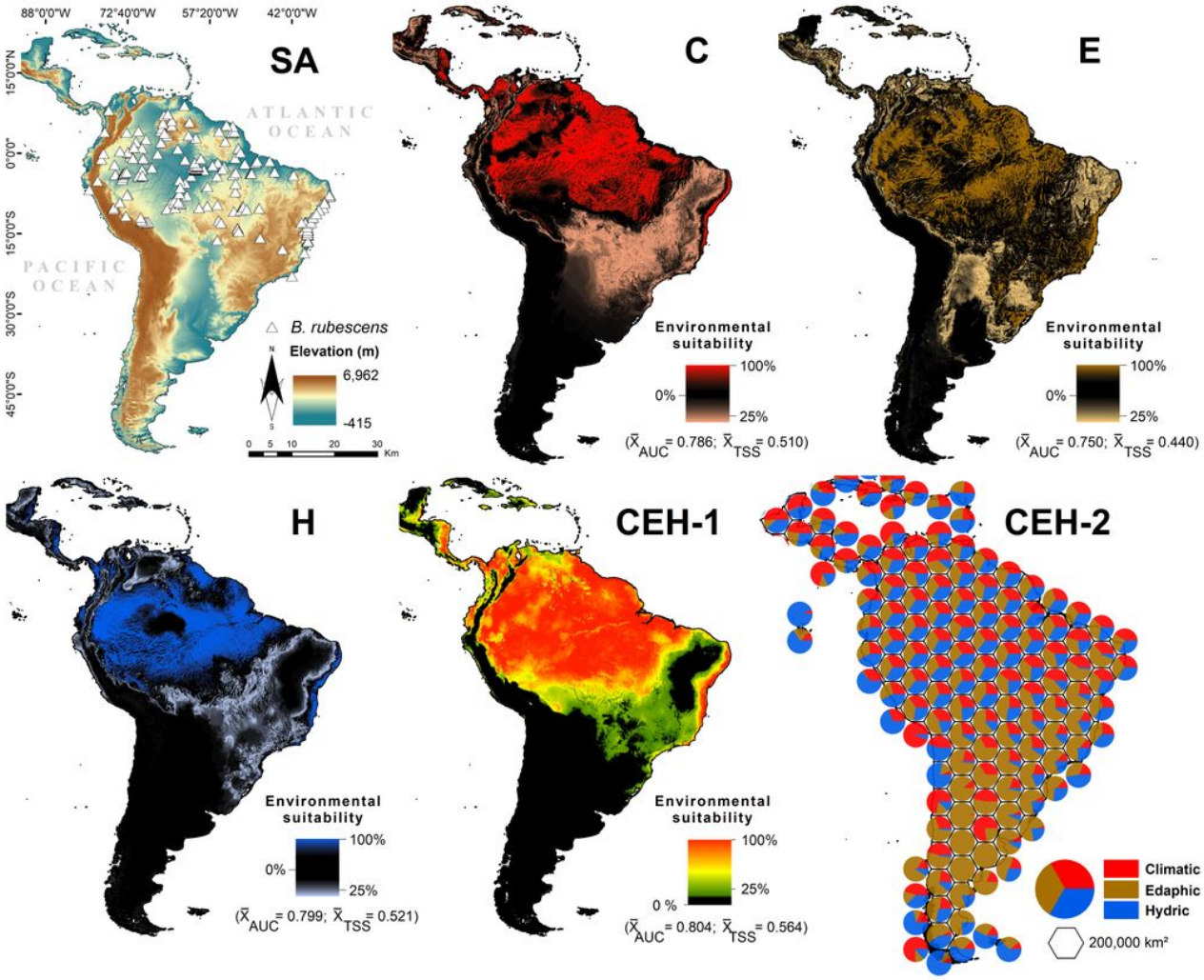

Figure 4

SDMs obtained for B. rubescens within the study area (SA - South America), against Climatic (C), Edaphic (E), Hydric (H) and all variables in a single PCA (CEH-1), the contribution graph of the variables acting together in space (CEH-2). With the corresponding values of mean AUC (Area Under the receiver-operator Curve) and TSS (True Skill Statistic) associated with each result Note: The designations employed and the presentation of the material on this map do not imply the expression of any opinion whatsoever on the part of Research Square concerning the legal status of any country, territory, city or area or of its authorities, or concerning the delimitation of its frontiers or boundaries. This map has been provided by the authors.

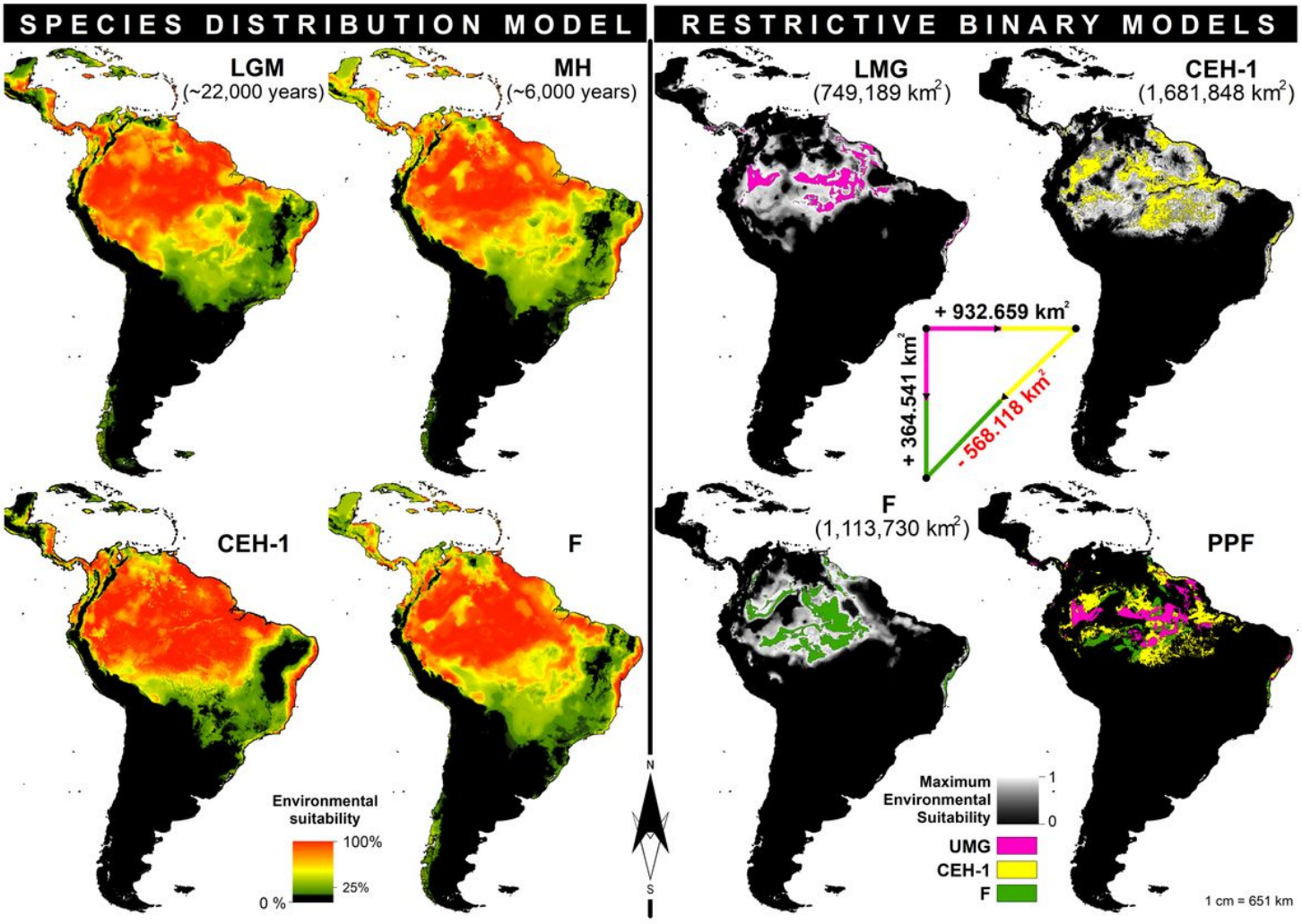

Figure 5

SDMs generated for B. rubescens from the LGM (Last Glacial Maximum), MH (Middle Holocene), Present (CEH-1), and Future (F) scenarios, accompanied by the values of AUC and TSS. On the right side, binary SDMs generated for the LGM, CEH-1, and F scenarios, where in grayscale the maximum values of environmental suitability can be observed, and in pink (LGM), yellow (CEH) -1) and green (F) suitability values equal to 1 (maximum or excellent predictions). And all the results of the binary SDMs together in PPF (Past, Present, and Future) representing the spatial overlap over time Note: The designations employed and the presentation of the material on this map do not imply the expression of any opinion whatsoever on the part of Research Square concerning the legal status of any country, territory, city or area or of its authorities, or concerning the delimitation of its frontiers or boundaries. This map has been provided by the authors.

Supplementary Files

This is a list of supplementary files associated with this preprint. Click to download.

- Supplementarymaterials.docx